

Aspects of Diffusive-Relaxation Dynamics with a Nonuniform, Partially Absorbing Boundary in General Porous Media

Seungoh Ryu and David Linton Johnson

Schlumberger Doll Research, One Hampshire Street, Cambridge, Massachusetts 02139, USA

(Received 10 March 2009; published 9 September 2009)

We consider the Helmholtz problem in the context of the evolution of uniform initial distribution of a physical attribute in general porous media subject to a partially absorbing boundary condition. Its spectral property as a reflection of the boundary geometry has been widely exploited, such as in biological and geophysical applications. We consider the situation where the critical assumptions which enable such applications break down. Specifically, what are the consequences of an inhomogeneous absorption strength? Using perturbation theory, exact theoretical results, and numerical simulations on random sphere packs, we identify the regions of parameter space in which such inhomogeneity is important and those in which it is not. Our findings shed light on the issue that limits the mapping between the diffusion or relaxation spectrum and the underlying boundary geometry.

DOI: 10.1103/PhysRevLett.103.118701

PACS numbers: 81.05.Rm, 76.60.-k, 89.90.+n, 91.60.-x

The spatiotemporal evolution of the density of an attribute carried by diffusing agents, subject to a partially absorbing boundary, occurs in a variety of scientific disciplines that ranges from NMR relaxometry in porous media [1,2] and biomedicine [3], waves in a membrane [4], to migration of genes and cultural influences [5]. In its minimal form, the problem is formulated as the Helmholtz problem, but in real systems, variations in the absorption strengths and local geometry complicate the matter, and changes in part of its spectrum or *phantom* length scales may appear [6]. Empirical data from such systems, usually lacking the reference system with which to compare, beg the question: Is such a feature inherent in the nature of the underlying dynamics (with a clean boundary) or due to the haphazard elements on it? We are directly motivated by NMR relaxometry in porous media in which issues of such nature have been long standing. We consider the situation where the draining strength, $\rho(\mathbf{r})$, varies from point to point on the boundary surface and probe how it intertwines with the boundary geometry. Although some studies exist on the aspects of the variable $\rho(\mathbf{r})$ [7–10], their systematic investigation is still lacking. In this Letter, we develop a theoretical framework which incorporates both effects on an equal footing by treating the spatial fluctuations of $\rho(\mathbf{r})$, $\delta\rho(\mathbf{r})$ as a perturbative parameter and identify the salient spectral consequences. The method is then applied to a simple problem, for which we obtain an exact solution for comparison. For realistic pore geometry and $\delta\rho(\mathbf{r})$ variations, we perform numerical simulations which show that the effect depends sensitively on the symmetry properties of both $\delta\rho(\mathbf{r})$ and the eigenmodes of the boundary-value problem associated with the uniform ρ .

We start with a generic and widely studied problem: the evolution of a local density $\Psi(\mathbf{r}, t)$ of a scalar attribute carried by entities diffusing (with diffusivity D) inside a general pore space (V_p) defined by the pore-matrix interface (Σ), which drains the attribute with a strength param-

eterized by the parameter $\rho_0(>0)$ upon contact. Defining the density operator as $\mathbf{J} \equiv -D(\mathbf{r})\nabla$ and $\mathcal{H} \equiv \nabla \cdot \mathbf{J}$, the local continuity of Ψ leads to the classic Helmholtz equation, and in seeking its solution in terms of the eigenmodes (i.e., $\{\phi_p^0(\mathbf{r})e^{-\lambda_p^0 t}\}$), one arrives at $\mathcal{H}\phi_p^0(\mathbf{r}) = \lambda_p^0\phi_p^0(\mathbf{r})$ ($p = 0, 1, \dots$) where each mode is subject to the Robin's condition $\hat{n} \cdot \mathbf{J}\phi_p(\mathbf{r}) = \rho_0\phi_p^0(\mathbf{r})$ on the boundary. We superscript λ_p^0 and ϕ_p^0 to indicate that it is for the uniform ρ_0 . From the properties of \mathcal{H} and ρ_0 , it follows that λ_p^0 are real and ≥ 0 ; orthonormal eigenmodes ϕ_p^0 can be represented as real functions. The connection between the spectrum of \mathcal{H} and the *boundary shape* (pore geometry) had been noted by Kac and others [11–13] and its various aspects have been explored in a variety of scientific disciplines [14–17]. In particular, the relaxation of polarized proton spins carried by fluid molecules in porous media such as rocks and biological samples is a pertinent example, as the relaxation is enhanced by the fluctuating dipole field near the interface [18,19]. The evolution of the total attribute (magnetization in the case of NMR) $\mathcal{M} \equiv \int_{V_p} d\mathbf{r}\Psi(\mathbf{r}, t)$, initially uniform, then follows $\mathcal{M}(t) = \sum_p e^{-\lambda_p t} |a_p^0|^2$ where $a_p^0 = \int_{V_p} \phi_p^0(\mathbf{r}) d\mathbf{r}$. In the case of a simple, closed boundary with a single defining length scale (such as the radius a in a spherical pore), this enhanced relaxation may be limited either by the strength of relaxation at the boundary or by the diffusivity D , and a control parameter $\kappa \equiv \rho_0 a/D$ emerges to separate the regimes which have distinct spectral properties (i.e., a_p and λ_p , $p = 0, 1, \dots$). In the limit where $\kappa \ll 1$, it was observed that $a_0 \sim 1$ for the slowest decay mode ($p = 0$), and also that $\lambda_0^0 = \rho_0 S/V_p$ ($= \rho_0 3/a$ for a sphere) directly proportional to the surface-to-volume ratio of the pore. In the other limit, faster modes generally gain in weight, and $\lambda_0^0 \sim \lambda_\infty \equiv D\pi^2/a^2$. In many situations, the relationship between λ_0^0 and S/V_p is exploited to map the observed spectral distribution $\{a_p\}$ to a distribution of pore

sizes. For this mapping to work, however, the pores should be isolated from each other, each satisfying the condition $\kappa \ll 1$, and finally ρ_0 should be uniform [6]. In most real porous media, the local variations in geometry and the strength of ρ (we will call the variation as its *texture* from now on) make it no longer feasible to characterize the dynamics with a single parameter κ . It is straightforward to show that, for an $\mathcal{M}(t)$ arising from a collection of pores distributed in sizes with uniform ρ (all satisfying $\kappa \ll 1$), one may as well construct an alternative model with pores of the same size but with an appropriately chosen range of ρ strengths. Furthermore, the pore space forms an extended, multiply connected manifold, with possible local variations in the diffusive-connectivity [20] of its constituents. It becomes increasingly inadequate to employ notions such as *pore sizes* and *throats*, analogous to the way one should progress from atomic orbitals to the band theory and further on to accommodate strong disorder in solid state physics. In this approach, a few properties of the eigenspectrum become key elements [21]. In the following, we seek to quantify how inhomogeneous $\rho(\mathbf{r})$ affects the spectral signatures and their experimental manifestation.

Let us first generalize the Helmholtz problem by substituting $\rho(\mathbf{r}) = \rho_0 + \delta\rho(\mathbf{r})$ for ρ_0 with the requirement $\oint_{\Sigma} \delta\rho(\mathbf{r}) d\sigma = 0$. Under this boundary condition, we pursue the new set of eigenmodes $\{\phi_p\}$ with eigenvalues λ_p . Using the self-adjointness of \mathcal{H} and Green's theorem, we obtain the following relationship [21,22]:

$$\lambda_p = \oint_{\Sigma} \rho(\mathbf{r}) |\phi_p(\mathbf{r})|^2 d\sigma + \int_{V_p} D(\mathbf{r}) |\nabla \phi_p(\mathbf{r})|^2 d\mathbf{r} \quad (1)$$

which expresses all eigenvalues as a sum of surface integral and the diffusion-controlled volume integral, analogous to the energy of a particle in a potential well given in terms of the potential and the kinetic part. The character of each eigenmode can be understood in terms of the competition between these two components. A general observation can be made for fast modes that the second component dominates and λ_p for $p > 0$ becomes progressively insensitive to ρ_0 and $\delta\rho$. We define $\kappa_p = \frac{\rho_0 \ell_p}{D}$ by introducing a length scale parameter for each mode $\ell_p \equiv \frac{\int d\mathbf{r} (\nabla \phi_p)^2}{\oint d\sigma (\nabla \phi_p)^2}$. Applied to the $p = 0$ mode, the criterion $\kappa_0 \ll$ or $\gg 1$ generalizes the earlier observations made for simple closed pore geometry [19] and is reminiscent of the Λ parameter for the electrical conductivity of pore filling fluid [23]. The spectral weight for the slowest mode a_0 is significantly weakened for $\kappa_0 \gg 1$, which leads to $\mathcal{M}(t)$ with a *multiexponential* characteristic that had invited the *potentially misleading* [6] interpretation based on isolated pore size distributions. Instead, we derive a relationship that shows that this weight is directly related to the spatial fluctuation of the slowest eigenmode:

$$|a_0|^2 = 1 - V_p \left(\int_{V_p} d\mathbf{r} |\phi_0(\mathbf{r})|^2 - \left| \int_{V_p} d\mathbf{r} \phi_0(\mathbf{r}) \right|^2 \right). \quad (2)$$

Note that these rigorous relationships [Eq. (1) and (2)] apply to general boundary shape and both uniform and inhomogeneous ρ . It is also straightforward to prove that slope of $\log \mathcal{M}(t)$ at early times should remain robust against the fluctuations $\delta\rho(\mathbf{r})$, $-\lim_{t \rightarrow 0} \frac{d}{dt} \log \mathcal{M}(t) \rightarrow \rho_0 \frac{\mathcal{S}}{V}$, but the range over which this is valid could be severely limited depending on the strength of $|\delta\rho|$. Many authors had considered the so-called mean lifetime $\tau = \sum_p a_p^2 / \lambda_p$ [2,7,8], for which we obtain $\tau = \tau_0 - \frac{1}{V_p} \times \oint_{\Sigma} d\sigma u_0^0(\mathbf{r}) \delta\rho(\mathbf{r}) u_0(\mathbf{r})$ where $u_0 \equiv \lim_{s \rightarrow 0} \int_0^{\infty} \Psi(\mathbf{r}, t) \times e^{-ts} dt$ with $\Psi(\mathbf{r}, t)$ being the local density under $\rho(\mathbf{r})$, and similarly with u_0^0 and Ψ_0 under the uniform ρ_0 .

The eigenvalue λ_0 and the spectral weight $|a_0|^2$ of the slowest mode are the most accessible indicator for the change in the boundary condition $\rho_0 \rightarrow \rho_0 + \delta\rho(\mathbf{r})$. In the following, we therefore focus on the fractional shift in the slowest eigenmode $\frac{\delta\lambda_0}{\lambda_0^0} \equiv \frac{\lambda_0 - \lambda_0^0}{\lambda_0^0}$ which determines the longtime slope of $\log \mathcal{M}(t)$ vs t . Figure 1 summarizes schematically these general observations. We first derive a perturbative solution for $\frac{\delta\lambda_0}{\lambda_0^0}$ for an arbitrary pore geometry and $\rho(\mathbf{r})$ texture, and compare the result with an exact solution. Assuming that the complete eigenmodes $\{\phi_p^0\}$ with λ_p^0 's are worked out already for the uniform ρ_0 , we put the eigenmodes for the new boundary condition with $\rho(\mathbf{r})$ as

$$\phi_p(\mathbf{r}) = c_p [\phi_p^0(\mathbf{r}) + \sum_{q \neq p} a_{pq} \phi_q^0(\mathbf{r})] + Q_p(\mathbf{r}) \quad (3)$$

where c_p is the normalization constant. We introduce the auxiliary function $Q_p(\mathbf{r}) \equiv \phi_p(\mathbf{r}) - \int d\mathbf{r}' \mathcal{P}(\mathbf{r}, \mathbf{r}') \phi_p(\mathbf{r}')$ using projection onto the Hilbert space spanned by the eigenmodes $\{\phi_p^0\}$ with uniform ρ_0 via $\mathcal{P}(\mathbf{r}, \mathbf{r}') = \sum_p \phi_p^0(\mathbf{r}') \phi_p^0(\mathbf{r})$. Note that formal inclusion of $Q_p(\mathbf{r})$ is necessary at this point to satisfy the $\rho(\mathbf{r})$ -boundary condition since ϕ_p , if it were to be spanned by $\{\phi_p^0\}$ alone, would only satisfy the uniform ρ_0 condition. Using the orthonormality of the complete sets $\{\phi_p\}$ and $\{\phi_p^0\}$, respectively, we

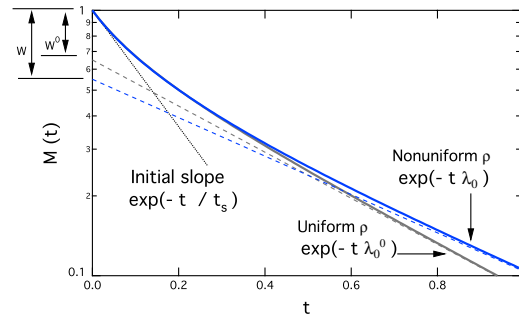


FIG. 1 (color online). Schematics for the difference between $\mathcal{M}(t)$ with a uniform and an inhomogeneous ρ with the final slopes given by λ_0^0 and λ_0 as indicated by the broken curves. The accompanying change in the spectral weight distribution is reflected in the difference between $W \equiv 1 - (a_0)^2$ and $W^0 \equiv 1 - (a_0^0)^2$.

obtain a recursive equation for a_{pq} :

$$a_{pq} = \frac{(1 - \delta_{pq})}{\lambda_p - \lambda_q^0} \left\{ \sum_r a_{pr} \delta \rho_{qr} + \delta \tilde{\rho}_{qp} \right\} \frac{S}{V_p} + \delta_{pq} \quad (4)$$

where we define overlap integrals $\delta \rho_{qr} \frac{S}{V_p} \equiv \oint_{\Sigma} d\sigma \phi_q^0 \delta \rho \phi_r^0$ and $\delta \tilde{\rho}_{qp} \frac{S}{V_p} \equiv \oint_{\Sigma} d\sigma \phi_q^0 \delta \rho Q_p$. Via iterative substitutions, we obtain the desired result in a systematic power expansion up to $\delta \rho^2$:

$$\lambda_p = \lambda_p^0 + \frac{S}{V_p} (\delta \rho_{pp} - \sum_{q \neq p} \frac{\delta \rho_{pq} \delta \rho_{qp}}{\lambda_q^0 - \lambda_p^0} \frac{S}{V_p} + \delta \tilde{\rho}_{pp}). \quad (5)$$

Defining $f_p(\mathbf{r}) \equiv \frac{1}{c_p} \sum_q \phi_q^0(\mathbf{r}) \oint_{\Sigma} d\sigma \phi_q^0 \delta \rho \phi_p^0$, a projection of $\delta \rho(\mathbf{r})$ spanned by $\{\phi_p^0\}$, we find that Q_p should satisfy the inhomogeneous equation: $(\mathcal{H} - \lambda_p)Q_p(\mathbf{r}) = f_p(\mathbf{r})$ subject to the condition $\rho_0 Q_p(\mathbf{r}) - \hat{n}(\mathbf{r}) \cdot \mathbf{J}Q_p(\mathbf{r}) = -\frac{1}{c_p} \delta \rho(\mathbf{r}) \phi_p^0(\mathbf{r})$ on the boundary. Note that $Q_p = [1 - \mathcal{P}] \phi_p$ may then be viewed as a superposition of waves with wavelength $\sqrt{D/\lambda_p}$ emanating from a surface localized source $[1 - \mathcal{P}] \delta \rho(\mathbf{r})$. For $p = 0$, our main focus, the effective source is averaged over a diffusion length $\sqrt{D/\lambda_0}$, as indicated by the presence of the $\lambda_p Q_p(\mathbf{r})$ term in its governing equation. This leads to $\delta \tilde{\rho}_{00} \sim 0$ as we find in the perturbative solution of the spherical pore [22]. For general pore geometry and $\rho(\mathbf{r})$ texture, we observe the following: Note that the first order term, $\delta \rho_{00}$, depends sensitively on the symmetry and the profile of the mode, $(\phi_0^0)^2$, along the boundary in relation to $\delta \rho$. While it vanishes for the simple situations where ϕ_0^0 is uniform along the boundary, it may not do so when there exists significant variation of ϕ_0^0 as when the complex pore geometry dictates. For empirical $\mathcal{M}(t)$ with a multiexponential characteristics, as often observed in geophysical applications [18], Eq. (2) suggests that one cannot safely assume $\phi_0^0(\mathbf{r})$ is uniform along the contours of the boundary. The strength of the first order contribution is further enhanced when the texture $\delta \rho(\mathbf{r})$ varies commensurate with $\phi_0^0(\mathbf{r})$ on the interface [6].

Now we turn to a spherical pore of radius a and seek exact solutions for both uniform ρ_0 and $\rho(\mathbf{r})$ of the form (with $\sigma \leq 1$) $\rho(\mathbf{r}) = \rho_0[1 + \sigma f(\theta)]$ where we consider the cases of a stepwise [$f(\theta < \pi/2) = -1, f(\theta \geq \pi/2) = 1$] and a sinusoidal [$f(\theta) = \cos(\theta)$] textures. We look for the eigenmodes [24] in the form of $\phi_k(\mathbf{r}) = \sum_{L=0}^{\infty} s_{k,L} j_L(kr) Y_L^0(\Omega)$ where $j_L(x)$ is the spherical Bessel function, Y_L^0 's are the spherical harmonic functions with $M = 0$ (due to the azimuthal symmetry). k represents an infinite set of numbers that allow for a nontrivial solution for the coefficients s_k that facilitate the boundary condition be met:

$$2\kappa \sum_L \Delta_{L,L'} j_L(ka) s_{k,L} - [j_{L'}(ka) + ka \{j_{L'+1}(ka) - j_{L'-1}(ka)\}] s_{k,L'} = 0 \quad (6)$$

where $\Delta_{L,L'} = \int d\Omega f(\theta) Y_L^0 Y_{L'}^0$. Viewed as a homogeneous

matrix equation $\mathcal{K} \cdot \mathbf{s}_k = 0$, the eigenvalues are found from the condition that $\det[\mathcal{K}] = 0$. We solve this by truncating the matrix to a finite, though large, size and searching numerically for the root. The fractional difference in the lowest eigenvalue ($\lambda_0 = Dk_{\min}^2$) between the uniform and nonuniform cases are shown in Fig. 2. First panel shows the *stepwise* texture with σ ranging from 0.01 to 1.0 as indicated. The results from both the exact solution (solid lines) and the second order perturbation (points) agree very well for $\kappa < 2$ for all values of σ , while for $\kappa > 2$, the agreement deteriorates progressively as σ grows beyond 0.5. λ_0 itself is shown in the second panel. An anomaly occurs in the $\kappa \gg 1$ limit with $\sigma = 1$ for which $\rho(\mathbf{r})$ vanishes on half of the hemisphere. In this special case, the limit $\kappa \gg 1$ acquires a new *diffusion-controlled* time scale (i.e., $\sim 1/\lambda_0$ is quadrupled from $\lambda_{\infty} = \frac{a^2}{D\pi^2}$ to $\lambda_{\infty}/4$, as the slowest mode is now controlled by diffusion from the $\rho = 0$ zone to the other end $\rho \rightarrow \infty$ over the distance of $2a$). This crossover is missing for the sinusoidal texture with $\sigma = 1$ (in the third panel) for which only a nodal point ($\theta = \pi$) exists on which $\rho(\mathbf{r})$ vanishes. This contrasting behavior is also verified in numerical simulations. Using the perturbative approach, it is now straightforward to incorporate more complicated $\rho(\mathbf{r})$ textures for small σ , using Fig. 2 as a guide for its validity.

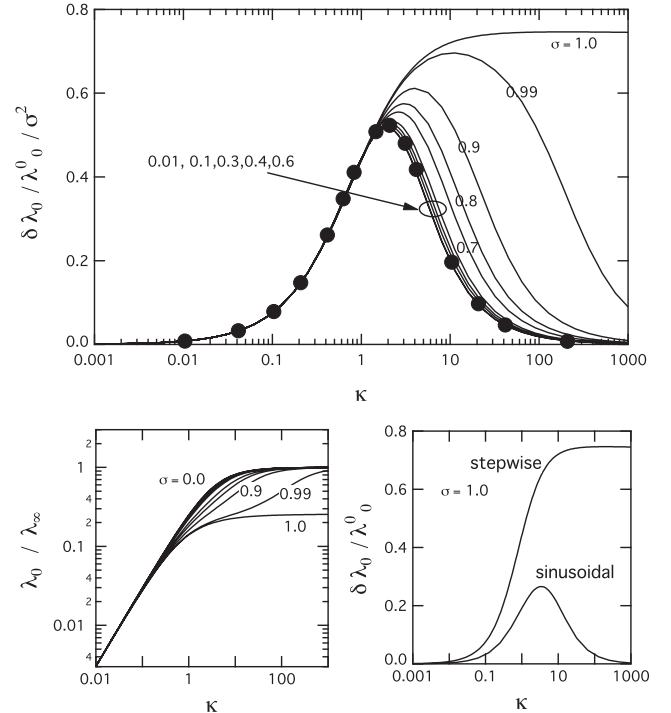


FIG. 2. Top: Results for a sphere of radius a and varying κ values with the hemispherical ρ texture. The solid lines show $\delta \lambda_0 / \lambda_0^0$ as obtained from the exact formulation described in the text. The filled points represent the second order perturbation result. Bottom left panel shows the $\lambda_0 / \lambda_{\infty}$ for varying σ 's as above. Bottom-right panel compares $\delta \lambda_0 / \lambda_0^0$ with $\sigma = 1.0$ for the hemispherical and the sinusoidal textures.

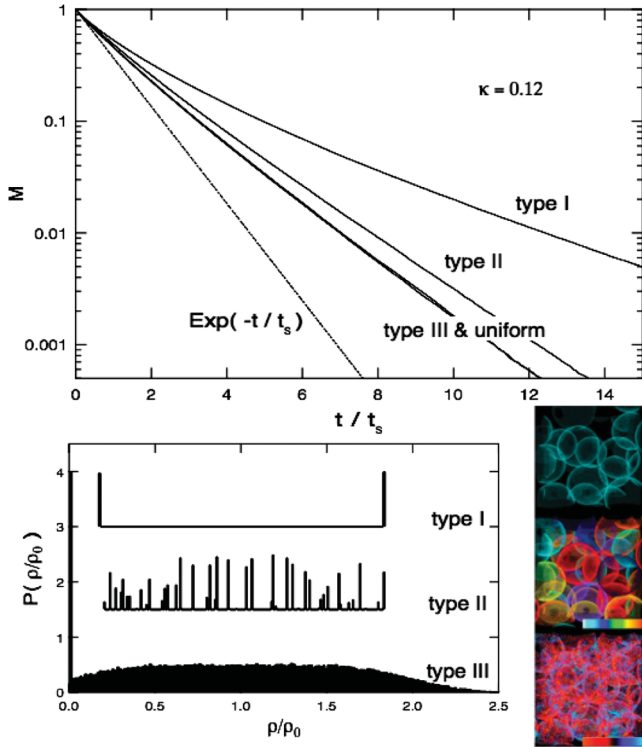


FIG. 3 (color). Top: Results for a Finney pack with three different ρ textures (all with $\rho_0 V_p/S/D = 0.12$) as well as with uniform ρ_0 for comparison. The broken line is an exponential function with the initial slope as expected with $1/t_s = \rho_0 S/V_p$.

Next, we consider the random glass bead pack as an example of realistic porous media for which well-controlled experiment and simulations could be carried out. Figure 3 shows the results from random walk simulations based on the Finney pack [25] in which we realize three different ρ textures that clearly violate the conditions necessary for the perturbative approach. Type I shows the strongest deviation from the uniform case (and is analogous to the case of the hemispherical ρ of Fig. 2 with $\sigma \sim 1$) as we randomly assign a value of 0.16 or $1.84 \times \rho_0$ to each grain with equal probability. In this case, $\delta\lambda_0/\lambda_0^0/\sigma^2 \sim 1.22$ is significantly larger than in the closed sphere even though $\kappa = 0.12$. This is likely due to the existence of wider spatial separations between the two ρ values, as expected in the pore morphology of a random packing. Type II draws randomly from a distribution of ρ values. Type III uses a texture generated using a correlated random noise [26]. In this case, values of $\delta\rho(\mathbf{r})$ are correlated over just a fraction of the bead radius, separating the correlations of boundary shape variation from that of $\delta\rho(\mathbf{r})$. Note that even though such $\delta\rho(\mathbf{r})$ has a wider distribution (bottom panels show the histogram and graphical rendition of each), the diffusive smearing greatly reduces its effect, and we obtain a result virtually indistinguishable from the uniform case. Similar observation had been made numerically by Valfouskaya *et al.* [9].

These textures cover a wide range of patterns relevant for natural media and applicable to bead packs [27] and other artificial structures [3].

We wish to acknowledge professor Adrianus T. de Hoop for useful discussions.

-
- [1] Y.-Q. Song, S. Ryu, and P. N. Sen, *Nature (London)* **406**, 178 (2000).
 - [2] D. S. Grebenkov, *Rev. Mod. Phys.* **79**, 1077 (2007).
 - [3] H. Lee, E. Sun, D. Ham, and R. Weissleder, *Nature Med.* **14**, 869 (2008).
 - [4] B. Sapoval, T. Gobron, and A. Margolina, *Phys. Rev. Lett.* **67**, 2974 (1991).
 - [5] J. Fort and V. Méndez, *Phys. Rev. Lett.* **82**, 867 (1999).
 - [6] S. Ryu, arXiv:0906.5327v1.
 - [7] D. J. Wilkinson, D. L. Johnson, and L. M. Schwartz, *Phys. Rev. B* **44**, 4960 (1991).
 - [8] A. R. Kansal and S. Torquato, *J. Chem. Phys.* **116**, 10589 (2002).
 - [9] A. Valfouskaya, P. M. Adler, J. F. Thovert, and M. Fleury, *J. Colloid Interface Sci.* **295**, 188 (2006).
 - [10] C. H. Arns, A. P. Sheppard, M. Saadatfar, and M. A. Knackstedt, *Proc. of the 47th Annual Logging Symposium (SPWLA, Houston 2006)*, p. 498610GG.
 - [11] M. Kac, *Am. Math. Mon.* **73**, 1 (1966).
 - [12] C. Gordon, D. L. Webb, and S. Wolpert, *Bull. Am. Math. Soc.* **27**, 134 (1992).
 - [13] S. J. Chapman, *Am. Math. Mon.* **102**, 124 (1995).
 - [14] B. Sapoval, M. Filoche, K. Karamanos, and R. Brizzi, *Eur. Phys. J. B* **9**, 739 (1999).
 - [15] P. G. de Gennes, *C. R. Acad. Sci. Paris, Ser. I* **295**, 1061 (1982).
 - [16] P. P. Mitra and P. N. Sen, *Phys. Rev. B* **45**, 143 (1992).
 - [17] M. Filoche, D. S. Grebenkov, J. S. Andrade, Jr., and B. Sapoval, *Proc. Natl. Acad. Sci. U.S.A.* **105**, 7636 (2008).
 - [18] R. L. Kleinberg, in *Encyclopedia of Nuclear Magnetic Resonance*, edited by D. M. Grant and R. K. Harris (John Wiley, Chichester, 1996).
 - [19] K. R. Brownstein and C. E. Tarr, *Phys. Rev. A* **19**, 2446 (1979).
 - [20] L. J. Zielinski, Y.-Q. Song, S. Ryu, and P. N. Sen, *J. Chem. Phys.* **117**, 5361 (2002).
 - [21] S. Ryu, *Magn. Reson. Imaging* **19**, 411 (2001).
 - [22] S. Ryu, *Phys. Rev. E* **80**, 026109 (2009).
 - [23] D. L. Johnson, J. Koplik, and L. M. Schwartz, *Phys. Rev. Lett.* **57**, 2564 (1986).
 - [24] D. L. Johnson and S. Ryu (unpublished).
 - [25] J. L. Finney, Ph.D. thesis, University of London, 1968. We used the subvolume of his bead pack for which each bead has a diameter of 50 voxels. Random walkers were deployed under the periodic boundary condition of the mirror-reflected volume in 256^3 voxels.
 - [26] S. Ryu, *Proceedings of the 49th Annual Logging Symposium (SPWLA, Houston, 2008)*, p. 737008 BB.
 - [27] S. Godefroy, J.-P. Korb, M. Fleury, and R. G. Bryant, *Phys. Rev. E* **64**, 021605 (2001).